Int. J. Solids Structures, 1968, Vol. 4, pp. 1161 to 1179. Pergamon Press. Printed in Great Britain

A FORMULATION AND SOLUTION PROCEDURE FOR THE GENERAL NON-HOMOGENEOUS ELASTIC INCLUSION PROBLEM

F. J. RIZZO and D. J. SHIPPY

University of Kentucky, Lexington, Kentucky

Abstract—A new formulation for the title problem, based on a fundamental solution of the equations of linear elasticity theory is described and exploited. The method is applicable without inherent restriction as to number, *shape*, and *material composition* of the inclusions which are embedded, in general, in a *finite* material matrix. Systems of singular integral equations arising from the fundamental solution are formed and solved numerically. Solutions to a number of test problems in two dimensions are given for illustration plus numerical data for two problems apparently heretofore unsolved.

INTRODUCTION

THE non-homogeneous inclusion problem, as referred to in the present work, is that associated with an arbitrary composite body described as follows: An isotropic elastic solid (material matrix) occupies a finite plane region and contains a number of isotropic elastic inhomogeneities as illustrated schematically in Fig. 1. The body is bounded by K

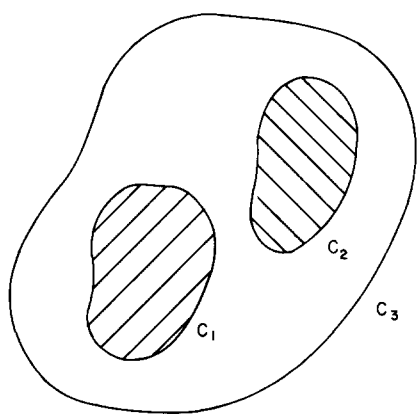

FIG. 1. Composite body $K = 3$.

smooth, non-intersecting contours C_ρ ($\rho = 1, 2, \ldots, K$), and the bonds across the inner contours are assumed inseparable.

The composite body is assumed to be stressed, in general, by a prescription of tractions or other suitable boundary data on the outer boundary of the matrix, C_K. In addition, a spontaneous expansion of one or more of the inhomogeneities is assumed to take place. The total stress and displacement fields in each portion of the composite body, due to *both*

conditions, are desired. Particular interest is attached to the vicinity of the contours C_ρ where stress concentrations are likely to arise. Two distinct cases occur: (1) no spontaneous expansion of the subregions takes place such that the entire internal effect is due to the boundary effort on C_K; or (2) C_K is traction free and a "locked-up" system of stress is achieved, due solely to the spontaneous expansion of subregion material. Case (1) is called the inhomogeneity problem whereas case (2) is referred to as the inclusion problem. This distinction coincides with terminology in the literature; however, limitations on the majority of practical approaches to such problems individually have precluded regarding them as special cases of a more *general* problem. Indeed, all available solutions to non-trivial inclusion problems (e.g. [1], [2], [3], [4], [5]) seem to require C_K to be indefinitely large, i.e., an infinite material matrix. Also, most solutions are available only for an inclusion of identical material composition as the matrix. References [1] and [3] are exceptions to this as will be discussed presently. In this work we formulate the general composite body problem at the outset. This includes, as sub-special cases, rigid inclusions, holes, as well as the general boundary value problem for a plane multiply-connected body, which arises, of course, when all subregions are free of material.

The method of solution involves K functional equations, defined on the body contours C_ρ, which are compatibility equations among the tractions across *and* displacements of points on C_ρ. Once boundary data on C_K plus the mismatch of contours which would take place if the inclusions could expand freely are prescribed, the functional equations become singular integral equations for the unknown mentioned tractions and displacements on C_ρ. These integral equations must be solved numerically in general but, as is shown, this can be done very effectively. Boundary stresses, e.g. the important discontinuous "hoop" stress, strain energies, plus field displacement and stress components are all found from a single computer program.

Specifically we solve the problem of an elliptic inclusion in an infinite matrix of different material and compare results with Jaswon and Bhargava [3] who use the complex variable formalism in conjunction with Eshelby's [6] point force method. The same problem by Bhargava and Radhakrishna [1] is solved using a standard energy method. It is important to note that the former's success is dependent on the uniformity of the stress field within an elliptic inclusion whereas the latter approach makes use of the fact that a relatively simple mapping function exists for the ellipse. No such restrictions are present here. We next solve the problem of the elliptic inclusion in a matrix with a finite circular outer boundary free of traction. In the absence of comparison data for this apparently unsolved problem, the validity of the solution is judged by the following schemes. The tractions on an imaginary circle surrounding the inclusion in the infinite matrix are computed and we place these on the boundary of the actual circle and compare results with the infinite matrix solution. This represents a check, in addition to demonstrating the capability of the method to, in fact, handle the combination or title problem. Also, a solution is obtained for the special ellipse, a circle, by a mere change of eccentricity which is checked against the analytical solution obtained by elementary means. Finally we examine the solution as the outer boundary of the matrix, free of traction, grows to approximate an infinite matrix.

The second problem we consider is the square inclusion in an infinite matrix. The presence of "corners" provides a stringent test of the method. Here, for different materials, a solution is again apparently unavailable. However, a trivial change in the value of Young's modulus on an input data card to the computer yields the solution for the homogeneous

inclusion. This then is compared with data from List and Silberstein [4] and Bhargava and Kapoor [2].

SOLUTION PROCEDURE

Let points on all contours be designated Q and let $t_i(Q)$* be the tractions exerted by the matrix on the inclusions across the boundaries C_ρ. The boundaries, at present, are assumed to have a continuously turning tangent everywhere. Tractions by the inclusions on the matrix are designated $s_i(Q)$ for which

$$t_i(Q)+s_i(Q) = 0 \qquad (\rho \neq K) \tag{1}$$

whereas $s_i(Q)$ on C_K is an applied external load. Further, regard the spontaneous expansion of the inclusions in the following hypothetical manner: Remove the inclusions from their positions in the body; allow them to expand or contract freely and denote the mismatch of the now separate contours as $\delta_i(Q)$; compress or expand them sufficiently to now make them fit their place in the stress free matrix; bond all contours securely and release the external effort such that the actual tractions across the bonds are the result of the mismatch (spontaneous expansion) plus whatever effort is due to the subsequent application of $s_i(Q)$ on C_K. Thus if $u_i(Q)$ and $v_i(Q)$ are the displacements of points on the free inclusion and matrix boundaries, respectively, then

$$u_i(Q)-v_i(Q) = \delta_i(Q) \qquad (\rho \neq K) \tag{2}$$

in which $\delta_i(Q)$ is the only known quantity. From a knowledge of $\delta_i(Q)$ on each contour plus $s_i(Q)$ on C_K, we wish to obtain an explicit field solution to the composite body problem.†

To this end consider the $K-1$ boundary functional equations, i.e. one for each inclusion as derived in [7],

$$u_j(P)+2\int_{C_\rho}[t_i(Q)U^\rho_{ij}(P,Q)-u_i(Q)T^\rho_{ij}(P,Q)]\,\mathrm{d}Q = 0 \qquad (\rho \neq K). \tag{3}$$

In these equations points P as well as Q are on C_ρ; U^ρ_{ij} and T^ρ_{ij} are fundamental tensors, singular when $P = Q$, derived from the point-force solution of the equations of elasticity (cf. [8] & [9]) and are listed for reference in the Appendix. The superscript ρ indicates dependence of these tensors on the material comprising the ρth inclusion; $\mathrm{d}Q$ is an element of arc length at point Q. The integration is performed keeping the inclusion on "the left", and the normal is taken positive outward. The analytical significance of equations (3) is that they ensure that both u_i and t_i on C_ρ correspond to the same arbitrary stress state present in the inclusion surrounded by C_ρ. The practical significance will be clear shortly. An additional equation referring to the matrix ($\rho = K$) may be written

$$v_j(P_\sigma)+2\int_L[s_i(Q)U^K_{ij}(P_\sigma,Q)-v_i(Q)T^K_{ij}(P_\sigma,Q)]\,\mathrm{d}Q = 0 \qquad (\sigma = 1,2,\ldots K) \tag{4}$$

* The indicial notation of Cartesian tensor analysis is used. Miniscule Latin subscripts have the range (1, 2) and for these the summation convention is implied. The range of Greek subscripts and superscripts is separately indicated.

† Body forces are assumed zero *et seq*.

in which the subscript σ indicates the specific contour occupied by the point P. The superscripts K indicate dependence on the material composition of the matrix and the integration is performed in the standard manner for a plane multiply-connected body, i.e., L is the contour C_K plus all the others traversed keeping the region in question, the matrix, on the left. Again, the normal points away from the region. Here, also, equation (4) ensures that both v_i and s_i on all contours refer to the same arbitrary stress state present in the matrix. Thus, equations (3) and (4) plus the coupling relations (1) and (2) are regarded as relations corresponding to a single compatible stress state for the composite body. Further, these relations are sufficient to determine all boundary tractions $t_i(Q)$, $s_i(Q)$ and all boundary displacements $u_i(Q)$, $v_i(Q)$, at all points Q from a specification *only* of $\delta_i(Q)$ on each C_ρ plus $s_i(Q)$ on C_K. Once all boundary functions are determined, displacement components and stress components may be obtained at an arbitrary *interior* point p_ρ by the integral identity

$$u_j(p_\rho) = \int_{C_\rho} [u_i(Q)T^\rho_{ij}(p_\rho, Q) - t_i(Q)U^\rho_{ij}(p_\rho, Q)]\, dQ \qquad (p \neq K) \tag{5}$$

and its derivatives according to

$$\tau_{jk}(p_\rho) = \lambda_\rho u_{i,i}(p_\rho)\delta_{jk} + \mu_\rho[u_{j,k}(p_\rho) + u_{k,j}(p_\rho)] \tag{6}$$

in which λ_ρ and μ_ρ are the usual Lamé constants and δ_{jk} is the Kronecker delta. Equation (5) is a Somigliana type integral (cf. [7], [8] and [9]) and identically satisfies the Navier–Cauchy equations for plane elastostatics. The stress field $\tau_{jk}(p_\rho)$ is derived from $u_j(p_\rho)$ as given by equation (5), noting that the derivatives affect only T^ρ_{ij} and U^ρ_{ij} since they are taken at p_ρ. If $\rho = K$, i.e., p_K is a point in the matrix, then replace $u_i(Q)$ by $v_i(Q)$ and $t_i(Q)$ by $s_i(Q)$ in equation (5) and extend the integrations over all contours as in equation (4).

It should be noted, before applying the above to an example, that if one or more of the inclusions are assumed rigid, relations of the type (3), strictly speaking, do not exist. However if the limit is taken as Young's modulus approaches infinity, the integrals involving U^ρ_{ij} go to zero. It may be shown (cf. [9]) that the equations which result, regarded as singular integral equations for the boundary displacements of a rigid inclusion, admit only the rigid body motion as might be expected. In practice, however, special attention is required only when there are two or more rigid inclusions. Specifically, setting $v_i(Q) = -\delta_i(Q)$ on the boundary of one inclusion completely determines the rigid body motion of the whole composite body. Thus the boundary conditions for the remaining rigid inclusions become

$$v_i(Q) = -\delta_i(Q) + a_i(Q) \tag{7}$$

in which $a_i(Q)$ is the movement of the associated rigid inclusion. This is determined in turn by the conditions that the tractions across that inclusion boundary are equilibrated. For such problems these conditions must be imposed, whereas in the general case of elastic inclusions they are automatically satisfied.

It is not to be inferred, however, that equation (4) requires $s_i(Q)$ on each C_ρ to be separately equilibrated. Indeed, if the material matrix to which equation (4) refers is the only body under investigation, i.e., an arbitrary multiply-connected body, data appropriate to a well-posed boundary value problem may be prescribed arbitrarily. The $s_i(Q)$ on any given contour, for example, need not be equilibrated; all that is required is that the whole body be in equilibrium. An example of this for a ring-shaped domain is given in [9]. In

short, the separate equilibrium of traction, as mentioned, is required merely for the definition of an inclusion and not for the validity of equation (4).

NUMERICAL TECHNIQUES

Explicit solutions to the general composite-body problem as posed are out of the question analytically, but an effective numerical attack may be made on equations (3) and (4) directly to find the unknown boundary functions. The basic scheme is as follows: Each contour C_ρ is divided into n_ρ selected intervals and within each interval a nodal point is located as shown in Fig. 2. Over any given interval, boundary tractions and displacements are assumed to be constant such that equation (3), for example, is approximated by the system

$$u_j(P_\eta)+2\sum_{\xi=1}^{n_\rho}\left\{t_i(Q_\xi)\int_\xi U_{ij}^\rho(P_\eta, Q)\,dQ-u_i(Q_\xi)\int_\xi T_{ij}^\rho(P_\eta, Q)\,dQ\right\}=0$$

$$(\eta = 1, 2, \ldots, n_\rho). \qquad (8)$$

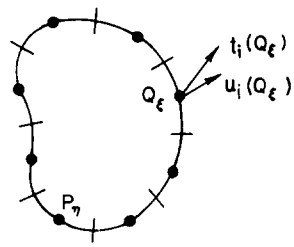

FIG. 2. Typical boundary approximation.

Unknowns are the discrete quantities $u_i(Q_\xi)$, $t_i(Q_\xi)$ associated with the nodes; and the integrations in (8), for a fixed choice of P_η, extend over each interval including that occupied by P_η itself. These integrals i.e.,

$$\int_\xi U_{ij}^\rho(P_\eta, Q)\,dQ, \qquad \int_\xi T_{ij}^\rho(P_\eta, Q)\,dQ \qquad (9)$$

are now regarded as known coefficients of the desired discrete displacement and traction components. The specific manner of performing such integrations for both cases, i.e., 1) P_η outside the interval of integration, and 2) P_η within the interval such that the corresponding integral is singular, is given in some detail in [9] for equations referring to a single "non-composite" body. The same scheme is adapted here with care taken to preserve the proper sense of integration appropriate to a given portion of the composite body and to use the different material constants. Thus the result of the boundary approximation is to replace the continuous system (3) by the discrete linear algebraic system (8). The system (8) may be written in more compact matrix form as

$$\mathbf{A}_\rho\mathbf{u}-\mathbf{B}_\rho\mathbf{t}=\mathbf{0} \qquad (\rho = 1, 2, \ldots, K-1) \qquad (10)$$

in which the matrices $\mathbf{A}_\rho$ and $\mathbf{B}_\rho$ are $2n_\rho$ square and contain all the mentioned integral coefficients. A similar reduction of equation (4) leads to the system

$$\mathbf{Dv}-\mathbf{Es}=\mathbf{0} \qquad (11)$$

in which $\mathbf{D}$ and $\mathbf{E}$ are $2N$ square with

$$N = \sum_{\rho=1}^{K} n_\rho.$$

Note that the matrices $\mathbf{A}_\rho$, $\mathbf{B}_\rho$, $\mathbf{D}$ and $\mathbf{E}$, above, *completely* characterize the size, shape and material composition of the composite body. Further, if any of these, e.g., $\mathbf{A}_\rho$, is partitioned into four parts

$$\mathbf{A}_\rho = \left[\begin{array}{c|c} \mathbf{A}_{\mathrm{II}} & \mathbf{A}_{\mathrm{I}} \\ \hline \mathbf{A}_{\mathrm{III}} & \mathbf{A}_{\mathrm{IV}} \end{array}\right]$$

the diagonal elements only of each part contain the principal values of the mentioned singular integrals. The way in which these and the other coefficients of $\mathbf{A}_\rho$ and $\mathbf{D}$ are obtained, using the fact that (cf. [9] and Appendix)

$$\int_{C_\rho} T_{ij}^{\rho}(P, Q)\, \mathrm{d}Q = \tfrac{1}{2}\delta_{ij}$$

assures singular $\mathbf{A}_\rho$ and $\mathbf{D}$ matrices. In fact, the rank of such matrices is three less than their size, as is required for the associated equations (10) and (11) to admit the three linearly independent rigid body freedoms. Thus in the discrete systems, the essential characteristics of the continuous systems (3) and (4) are maintained.

Consider, for definiteness, the problem of a single inclusion in an infinite matrix of different material. The parameter K is thus 2, with the outer boundary of the material matrix C_2 indefinitely large. The mismatch components δ_i are calculated for corresponding nodes on the contours of the matrix and inclusion, respectively, such that the array $\boldsymbol{\delta}$ of discrete $(2n_\rho)$ components is known. Now, since $s_i(Q)$ are equilibrated on the boundary C_1 and since the displacements vanish appropriately at infinity*, equations (4) and therefore equations (11) are written with P_σ and Q occupying only C_1. Incorporating (1) and (2) with equations (11) we have, for the material matrix

$$\mathbf{D}(\mathbf{u}-\boldsymbol{\delta})+\mathbf{E}\mathbf{t} = \mathbf{0} \tag{12}$$

and for the inclusion, the single relation

$$\mathbf{A}_1\mathbf{u}-\mathbf{B}_1\mathbf{t} = \mathbf{0}. \tag{13}$$

Thus, for the single inclusion in an infinite matrix there are a total of $4n_1$ equations in the $4n_1$ unknown displacements $\mathbf{u}$ and tractions $\mathbf{t}$ associated with the n_1 nodes on the common boundary. The combined system (12) and (13), for solution purposes may be written

$$\left[\begin{array}{c|c} \mathbf{A}_1 & -\mathbf{B}_1 \\ \hline \mathbf{D} & \mathbf{E} \end{array}\right]\left\{\begin{array}{c} \mathbf{u} \\ \hline \mathbf{t} \end{array}\right\} = \left\{\begin{array}{c} \mathbf{O} \\ \hline \mathbf{C} \end{array}\right\} \tag{14}$$

in which $\mathbf{C} = \mathbf{D}\boldsymbol{\delta}$ is known.

A considerable simplification is noteworthy when the inclusion and matrix are of the same material. In equations (10) and (11), the matrices $\mathbf{B}_1$ and $\mathbf{E}$ are identical and $\mathbf{A}_1$ and $\mathbf{D}$ are such that

$$\mathbf{A}_1+\mathbf{D} = 2\mathbf{I} \tag{15}$$

* These two conditions ensure the validity of equations (5) and (4) when C_K is indefinitely large (cf. [9]). Also, for this case, $\mathbf{D}$ in equation (11) is non-singular which assures that $\mathbf{v} = (\mathbf{u}-\boldsymbol{\delta})$ has a zero rigid body part.

where **I** is the identity matrix. Thus, the displacement components of the inclusion boundary are simply given by

$$\mathbf{u} = \tfrac{1}{2}\mathbf{D}\boldsymbol{\delta} \tag{16}$$

from which **t** may be obtained subsequently by

$$\mathbf{t} = \mathbf{B}_1^{-1}\mathbf{A}_1\mathbf{u}. \tag{17}$$

The results of (16) and (17) would follow, however, from a solution of (14) directly if preferred. In what follows, for generality (14) rather than (16), (17) was always used for computation of reported data for problems involving an infinite matrix regardless of the material composition.

TRIAL PROBLEM AND STRESS CALCULATIONS

As an illustration consider the (plane strain *et seq.*) problem of an elliptic inclusion in an infinite matrix. Figure 3 depicts a typical approximation of the inner boundary of the matrix. Nodes are equally spaced on the perimeter of the ellipse of semi-axes, a, b. A similarly situated elliptic inclusion of size $a(1+\varepsilon_1), b(1+\varepsilon_2)$ is assumed to exist and be fitted into the hole in the manner described earlier. Note that the physically important problem of a uniform thermal inclusion expansion is characterized by $\varepsilon_1 = \varepsilon_2$. An ellipse ratio $a/b = 2$ is chosen and the same material for matrix and inclusion is assumed. The non-homogeneous problem is discussed later in connection with a finite material matrix.

Three solutions were obtained for the trial problem, each involving a different number of nodes. In each case, node 1 is on the positive x_1-axis, with the other nodes numbered sequentially in a counterclockwise fashion as in Fig. 3. Data in the form of x_1-, x_2-components of displacement and traction on the inclusion boundary were obtained for each

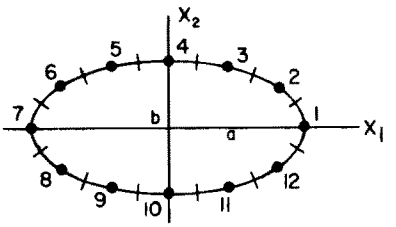

FIG. 3. Ellipse nodal pattern
$a/b = 2$; $n_1 = 12$.

value of n_1 and compared with analytical results from [3]. Such data for only the extreme points of the ellipse are given in Table 1. Computed data between the extremities are well behaved. Also, the analytical solution predicts uniform stress in the inclusion and zero dilatation in the matrix, which are verified by stress data reported subsequently.

Having achieved a boundary solution, i.e., **u** and **t** on C_1 for the elliptic inclusion, it remains to obtain the components of stress at the boundary C_1 in both the inclusion and matrix plus displacement components in the interior of both. In general, traction components t_i alone are insufficient to determine the stress state τ_{ij} in the inclusion at the boundary, but if u_i is known as well, its tangential derivative on C_1, i.e., $u_{i,s}$ is also known.

TABLE 1. HOMOGENEOUS ELLIPTICAL INCLUSION IN AN INFINITE MATRIX (TRIAL PROBLEM)*

	Displacements, u_i (in. $\times 10^{-2}$)		Tractions, t_i (psi $\times 10^4$)	
Node	u_1	u_2	t_1	t_2
	Numerical: $n_1 = 12$			
(x_1-axis) 1	−1·956	0	−1·266	0
(x_2-axis) 4	0	0·032	0	−0·710
	Numerical: $n_1 = 24$			
(x_1-axis) 1	−1·977	0	−1·436	0
(x_2-axis) 7	0	0·019	0	−0·730
	Numerical: $n_1 = 48$			
(x_1-axis) 1	−1·989	0	−1·483	0
(x_2-axis) 13	0	0·010	0	−0·740
	Analytical			
(x_1-axis)	−2·000	0	−1·500	0
(x_2-axis)	0	0	0	−0·750

* Semi-axis lengths: $a = 20$ in.; $b = 10$ in.
Young's modulus $= 10^7$ psi.
Poisson's ratio $= \frac{1}{3}$.
Mismatch parameter: $\varepsilon_1 = \varepsilon_2 = 2(10^{-3})$.

Thus the familiar relations on C_1, i.e.

$$\tau_{ij} = \lambda_1 u_{k,k}\delta_{ij} + \mu_1(u_{i,j} + u_{j,i}),$$
$$t_i = \tau_{ij} n_j, \qquad u_{i,s} = u_{i,j} q_j \tag{18}$$

in which n_j and q_j are unit normals and tangents, respectively, at Q, may be employed to determine τ_{ij} on C_1. For present purposes we may write

$$\mathbf{PJ} = \mathbf{M} \tag{19}$$

in which

$$\mathbf{J} = \begin{Bmatrix} \tau_{11} \\ \tau_{22} \\ \tau_{12} \\ u_{1,1} \\ u_{2,1} \\ u_{1,2} \\ u_{2,2} \end{Bmatrix} \quad \text{and} \quad \mathbf{M} = \begin{Bmatrix} 0 \\ t_1 \\ t_2 \\ 0 \\ u_{1,s} \\ 0 \\ u_{2,s} \end{Bmatrix}$$

The square matrix **P** contains the elastic constants and components of n_i, q_i arranged so as to have the single relation (19) represent the system (18). Thus, with these quantities arranged in a form for convenient computation, it is necessary to numerically obtain $u_{1,s}$ and $u_{2,s}$ at a given node Q. These derivatives plus t_1 and t_2 at Q complete the column **M** such that the stress components τ_{ij} on C_1 are obtained as the solution of (19) for each node. Along with the stresses, the displacement gradients $u_{i,j}$ are obtained, although the latter are not normally of interest. An identical system of the type (19) is defined using the variables for the material matrix to yield the corresponding stresses τ_{ij} on C_1. Numerical boundary stress data for the trial problem are given in Table 2 for the inclusion and in Table 3 for the infinite matrix, both for $n_1 = 48$. The proper discontinuity in hoop stress may be noted.

TABLE 2. BOUNDARY STRESSES IN ELLIPTICAL INCLUSION (TRIAL PROBLEM)

	Normal stresses (psi × 10^4)		Shear stress (psi × 10^4)	Hoop stress (psi × 10^4)
Node	τ_{11}	τ_{22}	τ_{12}	τ_H
Numerical: $n_1 = 48$				
(x_1-axis) 1	−1·484	−0·719	0	−0·719
(x_2-axis) 13	−1·491	−0·740	0	−1·491
Analytical				
(x_1-axis)	−1·500	−0·750	0	−0·750
(x_2-axis)	−1·500	−0·750	0	−1·500

TABLE 3. BOUNDARY STRESSES IN INFINITE MATRIX (TRIAL PROBLEM)

	Normal stresses (psi × 10^4)		Shear stress (psi × 10^4)	Hoop stress (psi × 10^4)
Node	τ_{11}	τ_{22}	τ_{12}	τ_H
Numerical: $n_1 = 48$				
(x_1-axis) 1	−1·484	1·475	0	1·475
(x_2-axis) 13	0·758	−0·740	0	0·758
Analytical				
(x_1-axis)	−1·500	1·500	0	1·500
(x_2-axis)	0·750	−0·750	0	0·750

A final quantity which may be obtained from the boundary solution alone is the strain energy in the composite body. In keeping with the approximation scheme this may be written

$$W_\rho = \tfrac{1}{2} \sum_{\xi=1}^{n_\rho} t_{i\xi} u_{i\xi} \Delta Q \tag{20}$$

for each inclusion or

$$W_K = \tfrac{1}{2} \sum_{\xi=1}^{N} s_{i\xi} v_{i\xi} \Delta Q$$

for the material matrix where ΔQ is the length of the ξth interval.

A now apparent feature of the present method of solution is that boundary traction, displacement, and stress components, plus the individual strain energies are obtainable *without* first achieving a complete *field* solution. In many, if not most, inclusion problems of engineering interest, only the above quantities are likely to be important. For such a case, nothing further need be calculated. Thus there is a certain efficiency and economy of effort built into the present scheme.

The final considerations in the present type of problem are the displacement and stress components in the interior of all regions as obtained by means of equations (5) and (6). The generation of the displacement field once the boundary solution is known is done via equation (5) written in the form

$$u_j(p_\rho) = \sum_{\xi=1}^{n_\rho} u_i(Q_\xi) \int_\xi T^\rho_{ij}(p_\rho, Q)\, dQ - \sum_{\xi=1}^{n_\rho} t_i(Q_\xi) \int_\xi U^\rho_{ij}(p_\rho, Q)\, dQ. \tag{21}$$

However, since the calculations present nothing new numerically and since the displacement field is less meaningful than the stress field for engineering purposes, it will not be discussed further. It suffices to remark that $u_j(p_\rho)$ may be obtained by means of equation (21), if desired, with accuracy comparable to that of all other reported quantities. The stress field, according to equation (6), is obtained by means of the expression

$$\begin{aligned}
\tau_{jk}(p_\rho) = \sum_{\xi=1}^{n_\rho} u_i(Q_\xi) \Big\{ & \lambda_\rho \delta_{jk} \int_\xi T^\rho_{im,m}(p_\rho, Q)\, dQ \\
& + \mu_\rho \int_\xi [T^\rho_{ij,k}(p_\rho, Q) - T^\rho_{ik,j}(p_\rho, Q)]\, dQ \Big\} \\
- \sum_{\xi=1}^{n_\rho} t_i(Q_\xi) \Big\{ & \lambda_\rho \delta_{jk} \int_\xi U^\rho_{im,m}(p_\rho, Q)\, dQ \\
& + \mu_\rho \int_\xi [U^\rho_{ij,k}(p_\rho, Q) - U^\rho_{ik,j}(p_\rho, Q)]\, dQ \Big\}
\end{aligned} \tag{22}$$

or in more compact matrix form

$$\tau_{jk}(p_\rho) = \mathbf{G}^\rho_{jk}\mathbf{u} + \mathbf{H}^\rho_{jk}\mathbf{t} \tag{23}$$

in which $\mathbf{G}^\rho_{jk}$ and $\mathbf{H}^\rho_{jk}$ are row matrices containing the indicated elements in curly brackets in equation (22). Thus, once p_ρ is specified, the row matrices may be calculated and τ_{jk} at p_ρ obtained by the simple matrix multiplication indicated.

Several operations in (22) and (23) should be emphasized. First, since p_ρ is an interior point, all integrals in (22) are non-singular. Further, note that T^ρ_{ij} can conveniently be written (see Appendix) as the tangential derivative of a suitable function, i.e.

$$T^\rho_{ij}(p_\rho, Q) \equiv \frac{d}{dQ} F^\rho_{ij}(p_\rho, Q).$$

Thus interchanging the order of differentiation we may integrate quantities of the form

$$\frac{\mathrm{d}}{\mathrm{d}Q} F^{\rho}_{ij,k}(p_\rho, Q)$$

over the ξth interval in (22) rather than $T^{\rho}_{ij,k}$ as written. Thus again we have an exact differential over the ξth interval and considerable accuracy is lent to the stress calculations by (22) and (23). Although a similar reduction to exact differentials is not possible with U^{ρ}_{ij} and its derivatives $U^{\rho}_{ij,k}$, the associated integrals are evaluated with good accuracy using a Simpson approximation. Finally, there is some question as to how close to the boundary p_ρ may be taken without possible difficulty with equation (22). Difficulty is expected very near C_ρ since the boundary is defined only by the coordinates of the nodes and interval points, and traction and displacement data are available only at the nodes. It has been found for all problems considered in this paper that p_ρ may be taken at least as close to C_ρ as the nodal spacing on C_ρ and still maintain ordinary accuracy, i.e., accuracy comparable to that available two or more nodal distances from C_ρ. Not being able to take p_ρ arbitrarily close to the boundary is not a limitation, however, since stresses *right on* the boundary, as already mentioned, may be obtained by the essentially independent process of equation (19).

Stresses interior to both the inclusion and the infinite matrix of the trial problem are given in Table 4 for points along the positive x_1-, and x_2-axes. The shear stress τ_{12} was found to be zero at all of those points as is predicted analytically [3]. Also, the stress field should be

TABLE 4. STRESSES IN INTERIOR OF ELLIPTICAL INCLUSION AND INFINITE MATRIX (TRIAL PROBLEM)

	Numerical: $n_t = 48$			
	Coordinates of point (in.)		Normal stresses (psi $\times 10^4$)	
	x_1	x_2	τ_{11}	τ_{22}
	0	0	−1·488	−0·739
	14	0	−1·484	−0·737
	16	0	−1·482	−0·735
	18	0	−1·484	−0·727
(Boundary of inclusion)	20	0	−1·484	−0·719
(Boundary of matrix)	20	0	−1·484	1·475
	22	0	−0·961	0·952
	24	0	−0·665	0·668
	26	0	−0·510	0·512
	40	0	−0·164	0·164
	0	4	−1·488	−0·739
	0	6	−1·489	−0·739
	0	8	−1·493	−0·734
(Boundary of inclusion)	0	10	−1·491	−0·740
(Boundary of matrix)	0	10	0·758	−0·740
	0	12	0·653	−0·658
	0	14	0·557	−0·558
	0	16	0·482	−0·483
	0	40	0·124	−0·124

uniform within the inclusion. Finally, $\tau_{11} = -\tau_{22}$ everywhere in the infinite matrix as expected.

Since the trial problem involves an elliptical inclusion of small eccentricity ($a/b = 2$), a reasonable concern is whether the present method works as well for inclusions of greater eccentricity (and thus greater curvature at the ends). To answer this question, two problems similar to the trial problem were solved, one with $a/b = 5$ and the other with $a/b = 10$. Numerical data from these solutions were found to compare as favorably with the corresponding analytical solutions as did the solution for $a/b = 2$ except right at the ends, where the curvature is greatest. There, for forty-eight nodes, the traction component t_1 (or stress component τ_{11}) deviated from the expected value at the ends by 19 per cent for the 5:1 ellipse and by 46 per cent for the 10:1 ellipse. However, in spite of the inaccuracy right at the extremities, the field stress is virtually unaffected; in fact, ordinary accuracy for all quantities is achieved everywhere except at the extremities. Unfortunately such points are often of most interest.

Thus, in an attempt to improve the accuracy right at the ends of the elongated ellipses, two adjustments were tried. Since any boundary, according to the present approximation scheme, is defined only by the coordinates of the nodal and interval points, the first attempt was to bunch the nodes and interval points toward the ends, keeping the total number of nodes for the whole boundary the same. In this way the part of the boundary with the greatest curvature was more accurately defined at the expense of the part relatively flat. Unfortunately, this procedure, which no longer admits equal spacing of nodes and equal interval lengths, impaired the conditioning of the algebraic equations. This impairment manifests itself in that certain columns of the coefficient matrices $\mathbf{A}_1, \mathbf{B}_1, \mathbf{D}, \mathbf{E}$ become orders of magnitude larger than before and tend to, improperly, dominate. Good conditioning was restored by examination of the matrices and scaling the appropriate columns before attempting to solve the equations. This reduced the error in t_1 at the ends to 6 per cent for the 10:1 ellipse. The scaling method, however, is still too laborious and untested to be a suggested procedure.

The second attempt was to merely increase the number of nodes and thus preserve equal spacing and good conditioning of the equations. Even though successful this procedure is much too inefficient if n_ρ is increased sufficient to obtain ordinary accuracy in the vicinity of extremely sharp curvature. The bunching procedure, in spite of the conditioning problem, is still the most sensible approach and is currently under more careful investigation. However, if we do not insist on information right at the "cusp" of the ellipse or other similar shape, it is possible to arrange the nodes straddling the cusp and locate an *interval* point instead at the cusp. This is the procedure used when a definite corner is encountered, as in the case of the square inclusion discussed in a later section of this paper.

ELLIPTIC INCLUSION IN FINITE MATRIX

A more complicated problem than that of the previous section involves an inclusion in a *finite* matrix; results are given for the particular problem of an elliptic inclusion in a matrix with a traction-free, circular outer boundary. To verify the solution, similar check problems to be described were solved.

The nodal pattern, with $n_1 = n_2 = 24$, used for the domain is shown in Fig. 4. The combination and simultaneous solution of equations (10) and (11) yield the 96 displacement components $\mathbf{v}$ at all the nodes plus the 48 traction components $\mathbf{s}$ across the nodes on

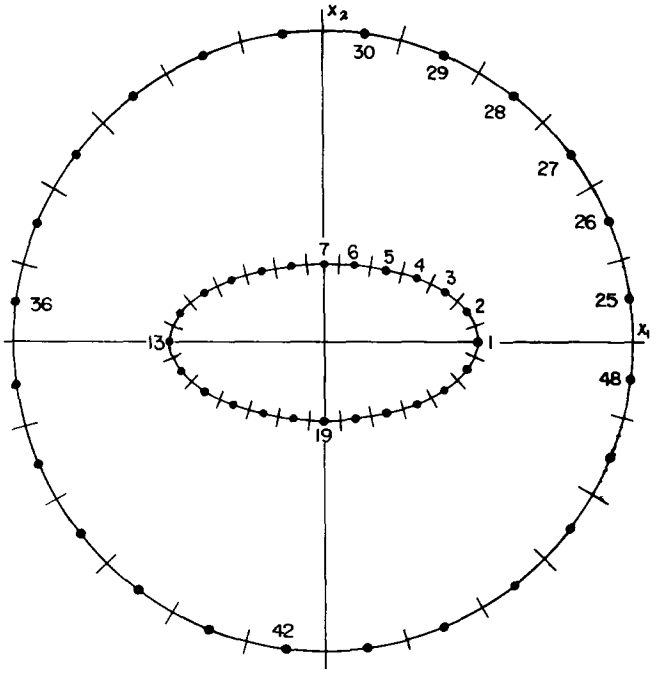

FIG. 4. Elliptic inclusion–finite circular matrix
$a/b = 2$, $R = 2a$, $n_1 = 24$, $n_2 = 24$.

the inner boundary. Note here that the matrices **D** and **E** refer to both inner and outer boundaries, since the latter is finite and hence **D** as well as $\mathbf{A}_1$ is singular. Thus it is necessary to specify the rigid body motion before attempting a simultaneous solution of (10) and (11). This is done by taking v_2 at nodes 1 and 13, v_1 at node 7 all zero (cf. Fig. 4) and thereby eliminating three algebraic equations from the total to be solved. Results for the traction-free outer boundary are given in Table 5 for all nodes in the first quadrant. Note that Young's modulus E for the matrix is three times that for the inclusion, illustrating the nonhomogeneous capability of the procedure.

To check the solution in the absence of analytical comparison data, we note the change in the data (reported for nodes 1 and 7 only) as the radius R grows; i.e. results for $R = 100$ in., $R = 10^4$ in., and finally, data for the infinite matrix are given in Table 5 together with analytical data from [1] for comparison. An additional check on the solution was obtained by merely specifying $a/b = 1$ as the ellipse parameter, i.e. a circular inclusion with $r = b$. Here the elementary analytical solution predicts $|v_i|_I = 1{\cdot}060(10^{-2})$ in., $|v_i|_O = 0{\cdot}340(10^{-2})$ in. everywhere on the inner and outer boundaries, respectively, and $|s_i| = 21{,}320$ psi as the traction across the junction of the two materials. This compares favorably with the values $|v_i|_I = 1{\cdot}041(10^{-2})$ in., $|v_i|_O = 0{\cdot}340(10^{-2})$ in., and $|s_i| = 21{,}520$ psi obtained numerically.

A final check on the non-homogeneous elliptic solution of Table 5 is obtained by computing the tractions occurring across an imaginary circle of radius $R = 40$ in. in the infinite matrix. This is done by obtaining the boundary solution for the infinite matrix and evaluating the stresses at points on the imaginary circle by means of equations (23). The corresponding tractions **s** easily obtained are then used in place of $\mathbf{s} = 0$ previously used on the circle. Results which agree well with the $R = \infty$ solution are reported in Table 6.

TABLE 5. NON-HOMOGENEOUS ELLIPTIC INCLUSION IN A FINITE CIRCULAR MATRIX*

		Displacements (in. × 10^{-2})		Tractions (psi × 10^4)	
Node		v_1	v_2	s_1	s_2
		$R = 40$ in.			
(x_1-axis)	1	1·013	0	2·307	0
	2	0·938	0·685	1·872	0·864
	3	0·782	1·168	1·243	1·177
	4	0·599	1·492	0·820	1·282
	5	0·405	1·703	0·502	1·327
	6	0·203	1·822	0·245	1·351
(x_2-axis)	7	0	1·862	0	1·352
	25	0·354	0·072	0	0
	26	0·415	0·251	0	0
	27	0·456	0·486	0	0
	28	0·416	0·728	0	0
	29	0·290	0·921	0	0
	30	0·104	1·027	0	0
		$R = 100$ in.			
	1	1·020	0	2·425	0
	7	0	1·687	0	1·612
		$R = 10^4$ in.			
	1	1·030	0	2·446	0
	7	0	1·649	0	1·665
		$R = \infty$			
	1	1·030	0	2·445	0
	7	0	1·649	0	1·664
		Analytical, $R = \infty$			
(x_1-axis)		1·000	0	2·531	0
(x_2-axis)		0	1·625	0	1·690

* Zero tractions on outer boundary.
Young's modulus for the inclusion = 10^7 psi.
Young's modulus for the matrix = $3(10^7)$ psi.
Poisson's ratio for inclusion and matrix = $\frac{1}{3}$.
Inclusion semi-axis lengths: $a = 20$ in.; $b = 10$ in.
Mismatch parameter: $\varepsilon_1 = \varepsilon_2 = 2(10^{-3})$.

TABLE 6. NON-HOMOGENEOUS ELLIPTIC INCLUSION IN A FINITE CIRCULAR MATRIX*

	Displacements (in. × 10^{-2})		Tractions (psi × 10^4)	
Node	v_1	v_2	s_1	s_2
1	1·030	0	2·447	0
7	0	1·649	0	1·661

* Non-zero tractions on outer boundary, $R = 40$ in.

SQUARE INCLUSION

A somewhat stringent test of the proposed method is provided by a square inclusion in an infinite matrix of different material. The key issue is the presence of *corners*; so although a rectangular inclusion could be handled easily enough, for convenience we consider only the square. Again, the relevant equations are identical to (14). The boundary nodal pattern for the first quadrant is shown in Fig. 5. Note that nodes coincident with the corners,

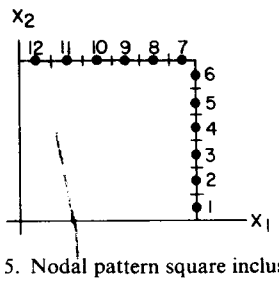

FIG. 5. Nodal pattern square inclusion (1st quadrant) $n_1 = 48$, equal spacing.

where no unique tangent exists, are avoided. This assures that equations (3) and (4) which lead to (14) are correct as written. If a point P in (3) or (4) were to occupy a corner, a factor involving the "angle" of the corner would appear instead of the simple factor "2" preceding the integrals (cf. [7]). Placement of nodes as indicated avoids such a modification. In order to compare results with [2] and [4], the solution for the homogeneous inclusion is obtained first. Results for the homogeneous problem and comparison data from [2] are given in Table 7. Because of symmetry, data are given only for the vertical half-side in the first quadrant. Note the absence of dilatation again in the infinite matrix.

A trivial change in the elastic constants for the inclusion, yielding different matrices $\mathbf{A}_1$, $\mathbf{B}_1$ in equation (14), results in the solution of a nonhomogeneous problem; these are given in Table 8.

The distortion of the half-sides of the inclusion as predicted by the numerical data is as shown in Fig. 6. Although only the maximum deflection was calculated from the lengthy formulas in [4] and was found to agree with the present solution, the general deformation pattern shown may be accepted with confidence since all the boundary stresses reported and verified are based on deflections as shown. However, the authors [2] show a pattern similar to Fig. 6(a), but with the inclusion deforming beyond its freely expanded position, i.e., the broken curve overlaps the dashed one over a portion of either half-side. This disagrees with [4], the present results, and the analytical expressions in [2] on which their drawings apparently are based. The pattern of Fig. 6(b) and the associated boundary stress data illustrate the expected changes due to an increase in inclusion stiffness to three times the matrix stiffness.

Note that reported data are good even for the node nearest the corner. This is in contrast to the situation recently reported by the authors [10], who use a different integral equation formulation to solve several plane boundary value problems of the theory of elasticity. In [10], the mere presence of corners causes ill-conditioning and fluctuating data over the entire boundary even with uniform nodal spacing. Thus, they must alter their boundaries by "rounding" the corners, i.e., replacing the two intervals adjoining the corners by arcs

TABLE 7. BOUNDARY STRESSES: HOMOGENEOUS SQUARE INCLUSION IN AN INFINITE MATRIX*

Numerical: $n_1 = 48$				
	Normal stress (psi × 10^4)	Tangential stress (psi × 10^4)	Inclusion hoop stress (psi × 10^4)	Matrix hoop stress (psi × 10^4)
Node	τ_{11}	τ_{12}	$\tau_H^{(I)}$	$\tau_H^{(M)}$
1	−0·619	−0·038	−1·148	0·630
2	−0·622	−0·116	−1·146	0·632
3	−0·626	−0·205	−1·141	0·637
4	−0·633	−0·314	−1·134	0·644
5	−0·643	−0·455	−1·132	0·645
6	−0·620	−0·956	−1·135	0·642
Analytical				
Node	τ_{11}	τ_{12}	$\tau_H^{(I)}$	$\tau_H^{(M)}$
1	−0·627	−0·038	−1·151	0·627
2	−0·629	−0·116	−1·148	0·629
3	−0·634	−0·205	−1·144	0·634
4	−0·641	−0·315	−1·136	0·641
5	−0·650	−0·472	−1·127	0·650
6	−0·661	−0·795	−1·117	0·661

* Young's modulus = 10^7 psi.
Poisson's ratio = $\frac{1}{4}$.
Half-length of side = 12 in.
Mismatch parameter: $\varepsilon_1 = \varepsilon_2 = 1/600$.

TABLE 8. BOUNDARY STRESSES: NON-HOMOGENEOUS SQUARE INCLUSION IN AN INFINITE MATRIX*

Numerical: $n_1 = 48$				
	Normal stress (psi × 10^4)	Tangential stress (psi × 10^4)	Inclusion hoop stress (psi × 10^4)	Matrix hoop stress (psi × 10^4)
Node	τ_{11}	τ_{12}	$\tau_H^{(I)}$	$\tau_H^{(M)}$
1	−0·716	−0·058	−1·587	1·090
2	−0·723	−0·179	−1·593	1·086
3	−0·738	−0·313	−1·608	1·078
4	−0·768	−0·480	−1·642	1·060
5	−0·820	−0·690	−1·734	1·018
6	−1·040	−1·508	−1·741	0·966

* Young's modulus for the inclusion = $3(10^7)$ psi.
Young's modulus for the matrix = 10^7 psi.

of circles. All singularities are thus removed. Such alterations of the contour are unnecessary here. The only modification employed here was in the computation of τ_{22} at the node closest to the corner. The procedure outlined in equation (19) requires the tangential

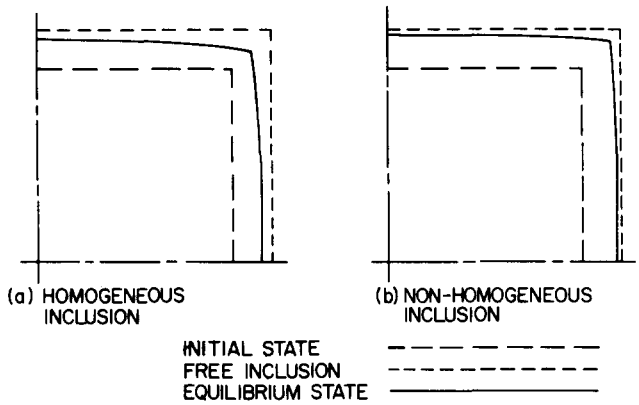

FIG. 6. Boundary configurations of one quadrant of square inclusion.

derivatives of u_i to be computed numerically. This is normally done simply by

$$\frac{u_{i(\xi+1)}-u_{(\xi-1)}}{|Q_{(\xi+1)}-Q_{(\xi-1)}|} \doteq u_{i,s}\Big|_{\xi\text{th node}}.$$

This simple scheme is bound to be ineffective when node ξ is closest to the corner since node $(\xi+1)$ is then "around the corner". However, it is an easy matter to determine $u_{i,s}$ more representatively for node ξ from a plot of the boundary displacement data and quickly calculate by hand the one component of stress, τ_{22}, which requires tangential derivatives of displacement for its determination.

CONCLUDING REMARKS

Several observations concerning the numerical procedures outlined are in order. First, all results were obtained taking advantage of symmetry. Specifically, elements of the coefficient matrices $\mathbf{A}_\rho$, $\mathbf{B}_\rho$, $\mathbf{D}$, $\mathbf{E}$ were obtained only for points P occupying positions in the first quadrant, such that only approximately one-quarter of the total number of algebraic equations indicated need be solved. The reduction is approximately $N/4$ since any nodes located at the ends of the first quadrant boundary or boundaries are always included (cf. Fig. 3). Even taking advantage of symmetry the available core storage capacity of the (IBM 360) computer would not be sufficient to allow doubling the number of nodes reported for the previous two problems. However, a significant feature of the present method is the good accuracy obtainable for a reasonably crude approximation of the boundary. Increases in n_ρ present no intrinsic problem if really necessary, but there is the disadvantage, with present facilities at least, of increasing computer time significantly over the five- to ten-minute maximums presently encountered. Also some experimentation with methods of solution of the algebraic equations may be necessary for much larger systems. Standard Gauss–Jordan and conjugate-gradient reduction schemes worked equally well for the present problems as reported. Instances of difficulty, i.e., corners or regions of continuously but rapidly changing curvature, both seem to require increases in node number and/or spacing changes, as described earlier, in order to obtain information *arbitrarily* close to

them. This is a tall order for any numerical scheme, but since the present one is, in principle, capable of providing such information, current work is directed toward effectively doing so.

The formulation itself, in terms of boundary tractions and displacements, is especially direct for inclusion problems. But it also possesses advantages for the special case of non-composite body problems over simpler formulations involving the biharmonic Airy function. Specifically, under the present system multivaluedness difficulties for multiply-connected domains are a priori eliminated. Further, only *first* derivatives of the field are required for stresses whereas second derivatives of the Airy function are necessary. Also, although the singular kernels in a biharmonic formulation (cf. [10]) are simpler in appearance, no terms may be integrated exactly over the boundary intervals. Thus less accuracy for a given nodal pattern is expected, not to mention additional difficulty with corners. Finally, *displacement* and *mixed* as well as traction-type boundary value problems for any single body may be attacked directly from equations (4) and (11) with no modification whatever.

An extension of the presented methods to problems involving material anisotropy is in its final stages. It has also been demonstrated in [11] and [12] that a boundary formula-singular integral formulation is possible and effective also for elasto*dynamic* problems. The present availability of the high capacity, high speed computer has resulted in considerable interest in singular integral formulations and numerical solutions of a variety of problems in mathematical physics. The papers [13], [14], [15], [16], [9], [10], [11] and [12] are perhaps only a sampling of such work.

Acknowledgements—One of the authors (F. J. R.) wishes to acknowledge partial support of the present study by the Graduate School of the University of Kentucky through the grant of a 1967 Summer Research Fellowship. Thanks are due also to M. Stippes for a valuable discussion. Finally, the authors gratefully acknowledge the generosity of the University of Kentucky Computing Center in making available an IBM 360 computer.

REFERENCES

[1] R. D. BHARGAVA and H. C. RADHAKRISHNA, Two-dimensional elliptic inclusions. *Proc. Camb. phil. Soc. math. phys. Sci.* **59** (1963).
[2] R. D. BHARGAVA and O. P. KAPOOR, Two-dimensional rectangular inclusion. *Proc. natn. Inst. Sci. India* (A), **32** (1966).
[3] M. A. JASWON and R. D. BHARGAVA, Two-dimensional elastic inclusion problems. *Proc. Camb. phil. Soc. math. phys. Sci.* **57** (1961).
[4] R. D. LIST and J. P. O. SILBERSTEIN, Two-dimensional elastic inclusion problems. *Proc. Camb. phil. Soc. math. phys. Sci.* **62** (1966).
[5] R. D. BHARGAVA and O. P. KAPOOR, Two-dimensional triangular inclusions in an elastic infinite medium. *Bull. Acad. pol. Sci. Sér. Sci. tech.* **11** (1963).
[6] J. D. ESHELBY, Elastic inclusions and inhomogeneities. *Proc. R. Soc.* **A376** (1959).
[7] F. RIZZO and M. STIPPES, Elastic inhomogeneity and inclusion problems. *Proc. 5th Mtg. Soc. Engng Sci.* (1967).
[8] A. E. H. LOVE, *A Treatise on the Mathematical Theory of Elasticity*, 4th edition. Dover (1944).
[9] F. RIZZO, An integral equation approach to boundary value problems of classical elastostatics. *Q. appl. Math.* **25** (1967).
[10] M. A. JASWON, M. MAITI and G. T. SYMM, Numerical biharmonic analysis and some applications. *Int. J. Solids Struct.* **3** (1967).
[11] T. A. CRUSE and F. J. RIZZO, A direct formulation and numerical solution of the general transient elastodynamic problem; I. *J. math. Analysis Applic.* **22** (1968).
[12] T. A. CRUSE, A direct formulation and numerical solution of the general transient elastodynamic problem; II. *J. math. Analysis Applic.* **22** (1968).
[13] M. A. JASWON and A. R. PONTER, An integral equation solution of the torsion problem. *Proc. R. Soc.* **273** (1963).

[14] G. T. SYMM, Integral equation methods is potential theory; II. *Proc. R. Soc.* **275** (1963).
[15] R. P. BANAUGH and W. GOLDSMITH, Diffraction of steady acoustic waves by surfaces of arbitrary shape. *J. acoust. Soc. Am.* **35** (1963).
[16] L. H. CHEN and D. G. SCHWEIKERT, Sound radiation from an arbitrary body. *J. acoust. Soc. Am.* **35** (1963).

APPENDIX

Fundamental tensors:

$$U_{ij}^{\rho} = \frac{(1+\nu_\rho)}{4\pi E_\rho(1-\nu_\rho)}\{(3-4\nu_\rho)\log r\delta_{ij} - r_{,i}r_{,j}\}$$

$$T_{ij}^{\rho} = \frac{1}{4\pi(1-\nu_\rho)}\left\{\frac{\partial}{\partial n}\log r[(1-2\nu_\rho)\delta_{ij} - 2r_{,i}r_{,j}] + (1-2\nu_\rho)[(\log r)_{,i}n_j - (\log r)_{,j}n_i]\right\}$$

ν_ρ = Poisson's Ratio

E_ρ = Young's Modulus

Note:

$$\frac{\partial}{\partial n}\log r \equiv \frac{\mathrm{d}\theta}{\mathrm{d}Q}, \qquad r = r(x_1'x_2'; x_1x_2)$$

$$r_{,1} = \cos\theta, \qquad r_{,2} = \sin\theta, \qquad \theta = \tan^{-1}\frac{x_2' - x_2}{x_1' - x_1}$$

(*Received* 4 *January* 1968; *revised* 31 *May* 1968)

Абстракт—Исходя из основного решения уравнений линейной теории упругости, приводится новая формулировка для задачи общего неоднородного упругого включения. Метод примененный без присущих ограничений как число, *форма* и *состав метериала* включений, находящихся в теле и вобще представлен в виде *конечной* матрицы козффициентов материала. Приводятся и решаются численно системы сингулярных интегральных уравнений, вытекающих из основного решения. Для иллюстрации даются решения для некоторого числа опытных задач в двух размерах, а также приводятся резуьтаты в явном виде для двух задач раньше нерешеных.